Current
Eye Research

Taylor & Francis
Taylor & Francis Group

Implementation of the Frequency Scatter Index in clinical commercially available double-pass systems

Journal:	*Current Eye Research*
Manuscript ID	NCER-2021-OR-0662
Manuscript Type:	Original Articles
Date Submitted by the Author:	15-Jul-2021
Complete List of Authors:	Sánchez, Roberto; Instituto de Investigación en Luz, Ambiente y Visión, García-Guerra, Carlos; Centre de Desenvolupament de Sensors, Instrumentació i Sistemes Martinez-Roda, Joan A.; Tech Univ Catalonia, Optics and Optometry de Paul, Aníbal; Instituto de Investigación en Luz, Ambiente y Visión Issolio, Luis; Departamento de Luminotecnia, Luz, Ambiente y Visión (DLLyV), ; Instituto de Investigación en Luz, Ambiente y Visión (ILAV-CONICET), Pujol, Jaume; Davalor Research Center - Universitat Politecnica de Catalunya
Keywords:	double-pass system, intraocular scattering, objective scatter index, frequency scatter index, cataracts

Implementation of the Frequency Scatter Index in clinical commercially available double-pass systems

Roberto F. Sánchez[a]*, Carlos E. García-Guerra[b], Joan A. Martínez-Roda[b], Aníbal G. de Paul[a], Luis A. Issolio[ac], and Jaume Pujol[b]

[a]*Instituto de Investigación en Luz, Ambiente y Visión, CONICET-UNT, Tucumán, Argentina;* [b]*Centre de Desenvolupament de Sensors, Instrumentació i Sistemes, Universitat Politecnica de Catalunya, Barcelona, España;* [c]*Departamento de Luminotecnia, Luz y Visión, Universidad Nacional de Tucumán, Tucumán, Argentina*

*corresponding author. Roberto Francisco Sánchez, Instituto de Investigación en Luz, Ambiente y Visión, Consejo Nacional de Investigaciones Científicas y Técnicas, Universidad Nacional de Tucumán, Av. Independencia 1800, San Miguel de Tucumán, Tucumán, Argentina. E-mail: rsanchez@herrera.unt.edu.ar

Implementation of the Frequency Scatter Index in clinical commercially available double-pass systems

Purpose: A previous work has reported a methodology to quantify intraocular scattering using a high sensitivity double-pass instrument with a robust index, the frequency scatter index (FSI). The purpose of our study was to evaluate an adaptation of the FSI for use in clinical double-pass systems.

Methods: A prospective observational study was carried out in a group of patients with nuclear cataracts (n=52) and in a control group (n=11) using conventional double-pass systems. The FSI and the objective scatter index (OSI) were used to assess the scattering. The Spearman coefficient was calculated to assess the correlation between OSI and FSI, obtained from the double-pass images. Simultaneous measurements were performed with a double-pass and with a Hartmann-Shack wavefront sensor in the control group. The root mean square wavefront error (RMS) and the full width at half maximum of the double-pass image (FWHM) were used to quantify the residual aberrations introduced by the variations in pupil size and retinal eccentricity.

Results: Measurement in eyes with different grades of cataracts shows a strong correlation (ρ=0.929, $p<0.0001$) between the FSI and the OSI. A certain degree of correlation was observed between the OSI and the RMS and between the OSI and the FWHM, both for measurements with a different pupillary diameter and with a different retinal eccentricity ($p<0.05$). No relationship was observed between the FSI and the RMS or between the FSI and the FWHM ($p>0.05$).

Conclusion: We have introduced and evaluated an adaptation of a methodology proposed recently for the measurement of intraocular scattering using the double-pass technique with a robust index, which is less affected by ocular aberrations. The FSI can be applied to conventional double-pass instruments available in clinical environments.

Keywords: double-pass system; intraocular scattering; objective scatter index; frequency scatter index; cataracts

Introduction

Intraocular scattering is a phenomenon produced by small structures in the optics of the eye that deviate incident light from a straight trajectory. In eyes with cataracts, the associated increment of forward scattering imposes a veiling illumination to the images formed onto the retina [1,2]. Consequently, the contrast, the brightness, and the quality of the retinal image may be affected [3-7]. In certain cases, common activities such as reading or night driving are compromised by image degradation [8]. In those cases, cataract gradation is relevant as this may be used by clinicians to evaluate whether cataract surgery is recommended.

Cataracts may be assessed with subjective techniques. For instance, clinicians consider aspects associated with backward scattering such as color, grade of opacification, and type of cataract from slit-lamp pictures to grade cataracts subjectively with the lens opacities classification system III (LOCS III) [9]. However, the visual performance is degraded by forward scattering, whose effects may differ from the effects produced by backward scattering depending on the size of the structures producing the cataract [10,11]. Forward scattering may be assessed with tests relying on the response of the patient. Examples of these techniques are the measurement of visual acuity on the presence of a glare source [12], the brightness comparison method that provides a glare index [13], or the use of the compensation-comparison method [14] implemented in the C-Quant instrument (Oculus Optikgeräte GmbH, Wetzlar-Dutenhofen, Germany).

Intraocular forward scattering may be objectively assessed with the double-pass technique using the objective scatter index (OSI) [15,16]. This metric compares the integrated light at an eccentric location with the one contained around the central position of the double-pass spot. The OSI is implemented in the clinical instrument HD

Analyzer (Visiometrics SL, Cerdanyola del Vallès, Spain) and has been used to classify cataracts [17,18]. However, the intraocular scattering quantification may be compromised under the presence of uncorrected refractive errors and higher-order aberrations [19,20]. To overcome such a limitation, the frequency scatter index3 (FSI_3) has been proposed [21]. This metric quantifies the effects of scattering at more eccentric locations of the double-pass image but analyzing the recorded data in the frequency domain. Although the FSI_3 is less affected by aberrations, this is computed from a double-pass image recorded with a 14-bit-depth scientific-grade camera. The high cost of this device may be a limitation to implement the index in clinical environments.

In this manuscript, we propose quantifying forward intraocular scattering using a modified version of the FSI_3. The index is called the frequency scatter index (FSI) and can be implemented in conventional double-pass instruments currently available in clinical environments, which are equipped with 8-bit-depth cameras. Besides introducing the FSI, this work also presents its validation. To do this, the FSI was used to quantify intraocular scattering in eyes with different grades of cataracts. In addition, the ability of the index to quantify scattering in conditions where aberrations present significant variations, such as different retinal eccentricities [22] or different pupillary diameters [23], was also tested.

Methods

The frequency scatter index3

It was proposed [21] to analyze the effects of intraocular scattering in the frequency domain using the ratio between a pair of modulation transfer functions (MTF) obtained from the same image, but considering two concentric square regions of interest of radii r1 ($MTF_{DP[r1]}$) and r2 ($MTF_{DP[r2]}$), with r1 < r2:

$$MTF_{DP[r2-r1]}(\nu) = \frac{MTF_{DP[r2]}(\nu)}{MTF_{DP[r1]}(\nu)} \quad (1)$$

To overcome the fact that differences in the extensions of the region of interest lead to MTFs with different resolutions, $MTF_{DP[r2\text{-}r1]}$ is evaluated only at frequencies ν that are common to both $MTF_{DP[r1]}$ and $MTF_{DP[r2]}$. In order to use the resolution provided by the smallest region of interest, the radii were defined in such a way that r2 was an integer multiple of r1.

In double-pass images, while aberrations affect mostly the region of the central peak (the central value especially), ocular scattering contributes to the intensity at more eccentric locations [16]. Thus, the radii in Eq. (1) have to be defined in such a way that the intensity in the region defined between r1 and r2 is mostly affected by scattering, but not by aberrations. Once the extensions of the regions are properly defined, the intraocular scattering may be quantified with FSI_3 as follows:

$$FSI_3 = \frac{n}{\sum_1^{n(\nu:\,3cpd)} MTF_{DP[r2-r1]}(\nu)} - 1 \quad (2)$$

where Σ stands for summation of the n common frequencies that exist between 0 and about 3 cycles per degree (cpd).

The frequency scatter index; a modification to FSI_3 to quantify forward scattering with clinical double-pass instruments

The FSI_3 was originally defined based on double-pass images recorded with an optical bench setup relying on a scientific-grade 14-bit-depth camera (16384 digital units). This property allowed the camera to detect the intensity variations produced by scattering within two regions of interest defined by r1=35.4 and r2=141 minutes of arc (arcmin)

with enough resolution. It has to be noted that this kind of technology is not available in commercial double-pass instruments, because of the high cost of such devices. Instead, the clinical double-pass systems are based on a camera that quantifies intensities using an 8-bit-depth (256 digital units). The recorded image is then used to estimate both the point spread function and the modulation transfer function using a region of interest with r=36.24 arcmin (256×256 pixels), a value approximately equal to the radius defining the smallest region of interest in the FSI_3. The differences in both the intensity resolution and the extensions of the region of interest make it impossible a direct implementation of the FSI_3 with conventional double-pass instruments such as those used currently in clinical practice.

Fig. 1 presents the radial profile of three double-pass images obtained with a commercial double-pass system. To obtain the profiles, six images were averaged for each subject and then a background image, recorded with a black diffusing background in place of the subject's eye, was subtracted from the average double-pass image. Then, to obtain the radial profile, an averaging was made in different meridians, with the center at the centroid of the double-pass image, in steps of one degree. Finally, for comparison reasons, the profiles were normalized to the unit. The curves correspond to healthy volunteers aged 22, 37, and 55 years with clear ocular media. As observed, the three curves present a decreasing trend with intensities very close to each other at the center of the images for eccentricities between 0 and about 15 arcmin. After this point, the highest intensities in the responses for the two older eyes indicate that the veil surrounding the double-pass spot associated with the increase of scattering with age starts to play a role at larger eccentricities [24]. On the other hand, the response for the youngest eye presents local fluctuations whose magnitude increases with eccentricity, probably because pixels quantizing low intensities as zero are considered during the

computation of the radial profile. Such behavior represents an undesired noise as a result of the low-intensity resolution of the recording device and the very low light power at such eccentricities in eyes without intraocular scattering. In the measured eye, for instance, this behavior becomes notorious after about 30 arcmin and makes the signal unreadable after about 60 arcmin. Based on these results, both the eccentricity at which the effects of intraocular scattering are noticed and the eccentricity at which the low-intensity resolution may become a restriction must be taken into account to define the region of interest used by the frequency scatter index (FSI) with clinical double-pass instruments.

We propose quantifying scattering with the FSI using 8-bit-depth images based on the analysis of two regions of interest of r1=17.98 (128×128 pixels) and r2=36.24 arcmin (256×256 pixels), and considering the first three common frequencies that are available between 0 and 3.28 cpd for the summation, where FSI is defined as follows:

$$FSI = \frac{3}{\sum_{1}^{:3cpd} MTF_{DP[36.24'-17.98']}(\nu)} - 1 \qquad (3)$$

We expect that the shorter extensions of r1 and r2 allow the camera to detect variations in intensity as a result of the scattering despite the loss in resolution. On the other hand, the lower values of the radii may lead to the effects of aberration being stronger than in the FSI_3. However, an FSI based on the analysis of two regions of interest with r1=17.98 and r2=36.24 arcmin should remain less affected by uncorrected aberrations than other metrics applied to double-pass images, like the OSI, which analyses a region between 12 and 20 arcmin.

Apparatus

For measures in patients with different grades of nuclear lens opacities, double-pass

images were obtained using two HD Analyzer systems at two different geographical locations. These commercially available clinical instruments provide double-pass images of 768×512 pixels with a resolution of 8.3 μm (0.285 arcmin) using an entrance and exit pupils of 2 and 4 mm, respectively, and a light source emitting at 780 nm.

To study the impact of increased aberrations on the FSI index due to increased pupil size and retinal eccentricity, a laboratory setup that incorporates a Hartmann-Shack (HS) wavefront sensor and a double-pass system was used (Fig. 2).

The apparatus consists of a modified double-pass system, with the second pass divided into two paths for simultaneous recording of double-pass and Hartmann-Shack images. For illumination, a filtered (ND, neutral density filter) infrared laser diode (MC7850CPWR-SMF, wavelength 785 nm) coupled to an optical fiber was used. The laser output forms a point-source object that is collimated by means of an aspheric lens (L1, 11 mm focal length), and a circular diaphragm (PE, φ=2 mm), conjugated with the eye pupil, completes the illumination path. A beam splitter (BS1) reflects 80% of the beam intensity, while the transmitted light is removed from the system by a light trap, LT. A Badal type optometer formed by two identical lenses (L2 and L3) of 200 mm in focal length and four mirrors (M1, M2, M3, and M4) was used to correct the refractive error of the subject. The correction was achieved after setting the proper optical distance between lenses L2 and L3 by moving horizontally the motorized platform on which mirrors M2 and M3 are mounted. The measuring branches are coupled to the assembly by the beam splitters BS2 (for the Hartmann-Shack sensor) and BS3 (for the double-pass system). After reflection in BS3, the light is collected with a lens (L4, 100 mm focal length) that forms the double-pass image on a CCD camera (UI-2220ME-M, IDS Imaging Development Systems GmbH, Germany), CCD DP. This 8-bit-depth camera recorded double-pass images with a pixel resolution of 8.3 μm (0.285 arcmin) using a

sensor of 768×576 pixels. A second diaphragm, PS, conjugated with PE acts as exit pupil. The light transmitted by BS3 (50R/50T) is then reflected by BS2 (70R/30T) and sampled by the microlens array (MLA, 0200-6.3-S-C, square geometry, 6.3 mm focal length, single microlens aperture of 200 μm). A CMOS camera (UI-1120SE-M-GL, IDS Imaging Development Systems GmbH, Germany), CMOS HS, placed at the focus location of the MLA records Hartmann-Shack images of 768×576 pixels with a resolution of 10 μm. The lenses L7 and L8, focal length 100 mm and 80 mm, respectively, form a telescope system with a magnification of -0.8, which makes it possible to measure pupils of up to 7 mm in diameter. For measuring the wave aberration in the eye pupil plane, MLA is conjugated with the eye pupil, and therefore the array is placed on the focus of lens L8, while diaphragms PE and PS are placed on the focus of lens L2.

The system permits setting the exit pupil of the instrument to 3, 4, 5, and 6 mm. When the Hartmann-Shack image is being processed, the wave aberration is estimated from the spots included in a circle that corresponds to the desired synthetic pupil. To produce the wave aberration over the double-pass exit pupil, the synthetic pupil has to be equal to or larger than this pupil. The subject head is placed on a chin rest on an XYZ positioning stage. During measurements, the camera CCD Pupil (UI-1221LE-M-GL, IDS Imaging Development Systems GmbH, Germany) monitored the alignment between the optical axis of the system and the pupil of the eye. The eye is illuminated at 900 nm by LEDs and the pupil plane is captured by a CCD sensor through lens L5 (f=50 mm), mirror M5, and a long-pass dichroic mirror (DM, 850 nm cut-on wavelength). This allows the pupil size to be correlated with the optical quality parameters measured with both sensors (Hartmann-Shack and double-pass) and control its shape during off-axis measurements. A fixation test (FT) located at the optical

infinity by lens L6 (f=100 mm) helps the subjects during the on-axis measurements. A horizontal panel located at 3 m from the observer with four red LEDs (angle subtended 5°, 10°, 15°, and 20°, respectively) was used as a fixation for measurements on the periphery.

The laser diode, cameras CCD DP, CMOS HS, and CCD Pupil, and the movement of the Badal by means of a stepper motor were controlled using a personal computer through a customized software developed in Visual Studio, while C#, EMGU CV, and a MATLAB script were used for image processing.

Subjects

We conducted a prospective study at two different locations in patients diagnosed with nuclear cataracts of different grades of nuclear lens opacity (NO2 to NO5 LOCS III grading) without any other ocular alteration (any eye disease other than cataract, surgical history, or pharmacological treatment were reasons for ruling out a patient). Fifty-two examinations were performed: 35 at the Ophthalmologic Service of Terrassa Hospital, and 17 at the Ophthalmologic Service of the National University of Tucumán. Also, 11 young healthy volunteers of the National University of Tucumán were considered as a control group. The inclusion criteria for the control group were corrected distance visual acuity of 20/20 or higher, spherical refraction in the range of -1.5 to +1.5 D, astigmatism less than -1.0 D, pupil diameter of 4 mm or greater under photopic conditions, and absence of a history of ocular diseases, surgery or pharmacological treatment.

A set of additional measurements was carried out in the 11 volunteers belonging to the control group. They were randomly divided into two groups: one group with seven subjects (Group1) for the measurements with different pupil sizes, and another

group of four subjects (Group2) for the measurements in fovea and periphery at different retinal eccentricities.

Ethical approval for this study was obtained from the Research Ethics Committee (CEI) of the National University of Tucumán and the National Council for Scientific and Technical Research (RESOLUCION N° 26/2018). Every patient and volunteer was informed about the topics of the study, and a written informed consent was obtained, following the tenets of the Declaration of Helsinki (Tokyo revision, 2004).

Experimental procedure

To evaluate the index for different grades of cataracts, the subjects of the cataract group and control group were measured with the clinical HD Analyzer system: first, the patient under assessment was well positioned and the refractive errors were internally corrected with the instrument; then, a scatter index measurement was executed. For each measurement, the instrument recorded six consecutive double-pass frames and the corresponding background image.

To analyze the impact of the aberrations, simultaneous double-pass and Hartmann-Shack measurements were performed in subjects of the Group1 with four different sizes of exit pupils (3, 4, 5, and 6 mm), and in subjects of the Group2 at five different eccentricity angles (0° (foveal), 5°, 10°, 15°, and 20°). In the foveal position, the fixation was made by observing the fixation test. In the measurements at different eccentricities, the subjects had to stare at the LED that was ON in the fixation panel. The measurements were taken after the subject was adapted to a dark room for 10 min to obtain a naturally dilated pupil, while the exit pupil of the system was controlled by the artificial diaphragm. In each record, six double-pass and Hartmann-Shack images,

and the corresponding background were taken per subject after correcting spherical refractive errors with the Badal system of the instrument.

During the acquisition time, the position of the pupil of the subject was monitored. Because centering the pupil with respect to the optical axis of the system is fundamental to avoid introducing errors in the measurement, whenever a movement was observed during the acquisition, the data were discarded and the measurement for that condition was repeated. Between each condition, the subject was asked to blink, avoiding the visualization of another light source. Blinking was necessary to avoid breaking the tear film during measurements, which would cause a worsening of the retinal image quality.

Data processing

In all cases, the FSI was calculated following the procedure described before (Eq. (3)). In the measurements of the cataract group and control group performed with the HD Analyzer system, the OSI value was provided by the clinical instrument. In subjects of Group1 and Group2, the OSI was computed from the recorded double-pass images. Besides, the root-mean-square wavefront error (RMS) computed from the Zernike coefficients was used as an indicator of the residual low and high order aberrations of the measured eye introduced by the variations in pupil size and retinal eccentricity. In the case of the double-pass images, the full-width at half-maximum (FWHM) was obtained as a metric to quantify the effects of uncorrected aberration during measurements [25]. In all the cases, the image used for the analysis was obtained by averaging the six available frames per measurement and the subsequent subtraction of the corresponding background image.

Statistical analysis

The Kolmogorov-Smirnov test was used to evaluate the normal distribution of the variables. An independent sample t-test was used to compare the control group and the eyes with cataracts. Because the OSI data did not meet the criteria for normal distribution, the Mann-Whitney U-test was used. The Spearman rank correlation coefficient (ρ) was calculated to assess the relationships between the variables studied. A linear generalized model (LGM) was used to analyze the linear growth slope of OSI and FSI with the increase of aberrations in repeated measurements at different retinal eccentricities and pupil diameters. Descriptive data are shown as the mean and standard deviation (SD) for normally distributed variables and as the median and interquartile range (IQR) for non-normally distributed variables. A value of $p<0.05$ was considered statistically significant.

Results

Frequency scatter index versus objective scatter index in eyes with cataracts

Fifty-two eyes of 52 patients diagnosed exclusively with nuclear cataracts were finally included in the analysis. The 35 patients from the Ophthalmologic Service of Terrassa Hospital were 55 to 86 years old (mean ± std: 69 ± 8 years; Female/Male: 20/15) and the 17 patients from the Ophthalmologic Service of the National University of Tucumán were 63 to 81 years old (mean ± std: 69 ± 7 years; Female/Male: 11/6). For individuals who had bilateral cataracts, only one eye (right or left) was randomly selected. No statistically significant differences were noted between the two samples regarding sex, age, OSI, or FSI. Eleven healthy eyes of 11 volunteers were considered as a control group (mean ± std: 32 ± 7 years; Female/Male: 5/6).

The FSI was significantly higher in the group with cataracts than in the control group ($p<0.0001$, $t=-7.919$, t-test), as expected, although that difference may also be very slightly attributable to the age difference between these groups. The OSI presented a similar behavior in these two groups ($p<0.0001$, $z=5.150$, Mann-Whitney U-test). Table 1 shows that as the LOCS III grade increases, so do both the OSI and the FSI. An analysis of variance (ANOVA) between grades of cataract scored with LOCS III showed statistically significant differences for FSI ($F=8.958$, $p<0.001$), in the same way as for OSI ($F=6.816$, $p<0.001$). However, the differences were not statistically significant between consecutive scores with Bonferroni post-hoc comparison.

A strong correlation was found between the FSI and the OSI ($\rho=0.929$, $p<0.0001$). Fig. 3 shows the scatter diagram for the FSI and OSI values.

Influence of pupil size and eccentricity

Tables 2 and 3 summarize the results of the Spearman rank correlation test with the ρ coefficient and the statistical significance p-value between the different parameters measured considering different pupil sizes in subjects of Group1 and different eccentricities from the fovea in subjects of Group2, respectively.

Some important considerations can be drawn from these tables. When changing the size of the exit pupil as well as the eccentricity of the double-pass spot from the fovea, a certain degree of correlation was observed between the OSI and the RMS of the wavefront (Fig. 4), as well as between the OSI and the FWHM of the double-pass image. As the ocular aberrations increase, the double-pass image degrades with a resulting increase in the width of the image, which explains the correlation between FWHM and RMS. In addition, no relationship was observed between the FSI and the

RMS (Fig. 4), or between the FSI and the FWHM, in any of the experiments carried out.

The increase in aberrations in the measurements is mostly a result of the increase in pupil size and the increase in eccentricity at the periphery of the fovea, depending on the experiment. When evaluating ocular media of healthy eyes without opacities, intraocular scattering is expected to remain low, and independent of aberrations. When the pupil size increases, a statistically significant increase in the OSI was observed (slope=0.123, p=0.0002, LGM), while there are no significant differences for the FSI values with the increase in pupil size (p=0.144, LGM). Similar behavior can be observed when increasing eccentricity; a statistically significant increase in the OSI was observed (slope=0.059, p=0.002, LGM), while there are no significant differences for the FSI values with the increase in eccentricity (p=0.611, LGM). Fig. 5 (A) shows a clear tendency to increase the average value of the OSI with the increase in the pupil size, while the FSI remains stable at a value close to 0.4 for all the pupils evaluated. Fig. 5 (B) also shows a marked increase in the OSI with eccentricity and greater stability of the FSI parameter.

Discussion

To overcome the limitation of the OSI for the quantification of intraocular scattering under the presence of uncorrected refractive errors and higher-order aberrations, the FSI_3 was recently proposed [21]. In the present work, we have studied the suitability of the proposed method to quantify forward intraocular scattering using conventional double-pass instruments currently available in clinical environments, which are equipped with 8-bits cameras, instead of the scientific-grade camera with 14-bits used during the definition of the FSI_3. This modified version is called the FSI, and it differs from the

FSI_3 in the extensions of the regions of interest chosen for the computation of the index.

In subjects with cataracts, both the FSI and the OSI increase with the LOCS III. The FSI is sensitive to scattering due to cataracts, even for the group of subjects graduated as NO2, where significant differences were found in the parameter compared to the control group ($p=0.0021$, $t=-3.761$, t-test). On the other hand, in our sample of subjects with cataracts OSI and FSI share approximately 85% of scattering (Fig. 3). It should be taken into account; however, that the sample tested corresponds to subjects diagnosed exclusively with nuclear cataracts and the results cannot be extrapolated to other types of cataracts, such as cortical or posterior subcapsular, as these have different patterns of scattering because of their morphology and location in the lens [17,26]. Hence, it would be worth expanding the study to determine the FSI values in patients with different types and degrees of severity of cataracts.

In this work a wavelength of 780 nm is used to measure the scattering as commercial equipment does, a choice which is justified by the comfort of the patient in a clinical environment. This scattering is a combination of the forward scattering with the scatter in the inner layers of the retina [27] because of the large penetration of infrared light used in both the experimental and the commercial double-pass systems. However, our results show that the effects of scattering due to the presence of an opaque medium, such as a cataract, are more notorious than possible variations amongst patients as a result of the scattering in the fundus at the working wavelength. Nevertheless, some differences may exist in the behavior of the FSI at wavelengths other than 780 nm.

During the calculation of the FSI, the area in which aberrations have a greater effect on the double-pass image is filtered and therefore such undesired effects are minimized. Previous works showed that an induced defocus on the double-pass image above 1 D results in a considerable overestimation of scattering as measured by OSI

[16,21]. Our results show that even a certain increase in aberrations as a result of daily life situations, such as the change in pupil size or peripheral vision, can affect the double-pass image significantly and therefore the value of the OSI while having little impact on the FSI when measuring scattering (Fig. 5). The lack of correlation between OSI and FSI in the measures with different eccentricities is probably attributable to the fact that in these measures the amount of aberrations is greater than that in the experiment with different pupil sizes (Table 2). This increase in aberrations resulted in a significant increase in OSI levels that are not reflected in the FSI. In this sense, the FSI parameter is more robust than the OSI.

Funding. This work was supported by the Consejo Nacional de Investigaciones Científicas y Técnicas (CONICET) under Grant number PUE 0114; Consejo de Investigaciones de la Universidad Nacional de Tucumán (CIUNT) under Grant number PIUNT E646; and Spanish Ministry of Science and Innovation (MICINN) under Grant number DPI2017-89414-R.

Declaration of interest statement. The authors declare no conflicts of interest.

Data availability. Data underlying the results presented in this paper are not publicly available at this time but may be obtained from the authors upon reasonable request.

References

1. Holladay LL. The fundamentals of glare and visibility. J Opt Soc Am. 1926;12(4):271-319.
2. Navarro R. Incorporation of intraocular scattering in schematic eye models. J Opt Soc Am A. 1985;2(11):1891-1894.

3. Williams DR, Brainard DH, McMahon MJ, Navarro R. Double-pass and interferometric measures of the optical quality of the eye. J Opt Soc Am A. 1994;11(12):3123-3135.
4. Westheimer G, Liang J. Influence of ocular light scatter on the eye's optical performance. J Opt Soc Am A. 1995;12(7):1417-1424.
5. Cox MJ, Atchison DA, Scott DH. Scatter and its implications for the measurement of optical image quality in human eyes. Optom Vis Sci. 2003;80(1):58-68.
6. Díaz-Doutón F, Benito A, Pujol J, Arjona M, Güell JL, Artal P. Comparison of the retinal image quality with a Hartmann-Shack wavefront sensor and a double-pass instrument. Invest Ophthalmol Vis Sci. 2006;47(4):1710-1716.
7. Issolio L, Barrionuevo P, Comastri S, Colombo E. Veiling luminance as a descriptor of brightness reduction caused by transient glare. J Opt Soc Am A Opt Image Sci Vis. 2012;29(10):2230-2236.
8. Morris D, Fraser SG, Gray C. Cataract surgery and quality of life implications. Clin Interv Aging. 2007;2(1):105-108.
9. Chylack Jr LT, Wolfe JK, Singer DM, Leske MC, Bullimore MA, Bailey IL, Friend J, McCarthy D, Wu SY. The Lens Opacities Classification System III. The longitudinal study of cataract study group. Arch Ophthalmol. 1993;111(6):831-836.
10. Bettelheim FA, Ali S. Light scattering of normal human lens III. Relationship between forward and back scatter of whole excised lenses. Exp Eye Res. 1985;41(1):1-9.
11. Beckman C, Nilsson O, Paulsson LE. Intraocular light scattering in vision, artistic painting, and photography. Appl Opt. 1994;33(21):4749-4753.
12. Bailey IL, Bullimore MA. A new test for the evaluation of disability glare. Optom Vis Sci. 1991;68(12):911-917.

13. Barrionuevo PA, Colombo EM, Vilaseca M, Pujol J, Issolio LA. Comparison between an objective and a psychophysical method for the evaluation of intraocular light scattering. J Opt Soc Am A. 2012;29(7):1293-1298.
14. Franssen L, Coppens JE, van den Berg TJ. Compensation comparison method for assessment of retinal straylight. Invest Ophthalmol Vis Sci. 2006;47(2):768-776.
15. Güell JL, Pujol J, Arjona M, Díaz-Doutón F, P. Artal P. Optical Quality Analysis System; Instrument for objective clinical evaluation of ocular optical quality. J Cataract Refract Surg. 2004;30(7):1598-1599.
16. Artal P, Benito A, Pérez GM, Alcón E, de Casas A, Pujol J, Marín JM. An objective scatter index based on double-pass retinal images of a point source to classify cataracts. PLoS One. 2011;6(2):e16823.
17. Vilaseca M, Romero MJ, Arjona M, Luque SO, Ondategui JC, Salvador A, Güell JL, Artal P, Pujol J. Grading nuclear, cortical and posterior subcapsular cataracts using an objective scatter index measured with a double-pass system. Br J Ophthalmol. 2012;96(9):1204-1210.
18. Filgueira CP, Sánchez RF, Colombo EM, Vilaseca M, Pujol J, Issolio LA. Discrimination between surgical and nonsurgical nuclear cataracts based on ROC analysis. Curr Eye Res. 2014;39(12):1187-1193.
19. Miao H, Tian M, He L, Zhao J, Mo X, Zhou X. Objective optical quality and intraocular scattering in myopic adults. Invest Ophthalmol Vis Sci. 2014;55(9):5582-5587.
20. Zhao J, Xiao F, Kang J, Zhao H, Dai Y, Zhang Y. Quantifying intraocular scatter with near diffraction-limited double-pass point spread function. Biomed Opt Express. 2016;7(11):4595-4604.

21. Martínez-Roda JA, García-Guerra CE, Díaz-Doutón F, Pujol J, Salvador A, Vilaseca M. Quantification of forward scattering based on the analysis of double-pass images in the frequency domain. Acta Ophthalmol. 2019;97(7):1019-1026.
22. Navarro R, Artal P, Williams DR. Modulation transfer of the human eye as a function of eccentricity. J Opt Soc Am A. 1993;10(2):201-212.
23. Artal P, Navarro R. Monochromatic modulation transfer function of the human eye for different pupil diameters: an analytical expression. J Opt Soc Am A. 1994;11(1):246-249.
24. Martínez-Roda JA, Vilaseca M, Ondategui JC, Aguirre M, Pujol J. Effects of aging on optical quality and visual function. Clin Exp Optom. 2016;99(6):518-525.
25. Logean E, Dalimier E, Dainty C. Measured double-pass intensity point-spread function after adaptive optics correction of ocular aberrations. Opt Express. 2008;16(22):17348-17357.
26. Paz Filgueira C, Sánchez RF, Issolio LA, Colombo EM. Straylight and visual quality on early nuclear and posterior subcapsular cataracts. Curr Eye Res. 2016;41(9):1209-1215.
27. Berendschot TT, DeLint PJ, van Norren D. Fundus reflectance-historical and present ideas. Prog Retin Eye Res. 2003;22(2):171-200.

Table 1. FSI and OSI values of the control and cataract groups.

Parameter	Control group	Subgroups of LOCS III grade			
		NO2	NO3	NO4	NO5
OSI Median (IQR)	0.46 (0.10)	1.83 (2.68)	2.83 (3.78)	3.87 (3.77)	4.35 (4.76)
FSI Mean (SD)	0.42 (0.09)	0.64 (0.13)	0.66 (0.19)	0.76 (0.19)	0.80 (0.16)

FSI, frequency scatter index; OSI, objective scatter index; IQR, interquartile range; SD, standard deviation; NO, nuclear opalescence; LOCS, lens opacities classification system.

Table 2. Spearman rank correlation coefficient (ρ) and p-value for the data of Group1 with different pupil sizes.

	ρ (p-value)		
	OSI	FSI	RMS
FSI	0.545* (0.0033)		
RMS	0.475* (0.0124)	-0.039 (0.8477)	
FWHM	0.822* (<0.0001)	0.199 (0.3188)	0.582* (0.0014)

*Correlation is significant at the 0.05 level. FSI, frequency scatter index; OSI, objective scatter index; RMS, root mean square of wavefront error; FWHM, full width at half maximum.

Table 3. Spearman rank correlation coefficient (ρ) and p-value for the data of Group2 with different retinal eccentricities.

	ρ (p-value)		
	OSI	FSI	RMS
FSI	0.213 (0.3680)		
RMS	0.476* (0.0338)	0.043 (0.8570)	
FWHM	0.475* (0.0342)	-0.099 (0.6758)	0.388 (0.0910)

*Correlation is significant at the 0.05 level. FSI, frequency scatter index; OSI, objective scatter index; RMS, root mean square of wavefront error; FWHM, full width at half maximum.

Figure 1. Normalized intensity in logarithm scale of the radial profiles of double-pass images for three subjects of 22 (black), 37 (light grey), and 55 (dark grey) years recorded with a commercial double-pass system. The region between grey dashed lines is used by the objective scatter index (OSI) and the region between black dashed lines is used by the frequency scatter index (FSI).

Figure 2. Layout of the double-pass setup to analyze the impact of aberrations. PE, entrance pupil; PS, exit pupil; BS, beam splitter; L, lens; M, mirror; Laser, laser diode; CCD, CCD camera; CMOS, CMOS camera; MLA, microlens array; DM, dichroic mirror; ND, neutral filter; FT, fixation test; PH, pinhole; LT, light trap; IR LED, Infrared light-emitting diode. In dark grey, the optical path of the first pass; in light grey, the optical path of the second pass.

Figure 3. Dispersion diagram for the frequency scatter index versus the objective scatter index. Data correspond to subjects with diagnosed nuclear cataracts and subjects of the control group. The straight line was fitted through least squares (R^2=0.85).

Figure 4. Objective scatter index (OSI) and frequency scatter index (FSI) as a function of the RMS of the wavefront when the pupil size increases (A) and when the eccentricity increases (B). Squares correspond to OSI and triangles to FSI. The straight line is a fit through least squares.

Figure 5. Mean value of the objective scatter index (OSI, squares) and frequency scatter index (FSI, triangles) for each pupil size (A) and eccentricity (B) evaluated in normal subjects. Error bars correspond to standard error.

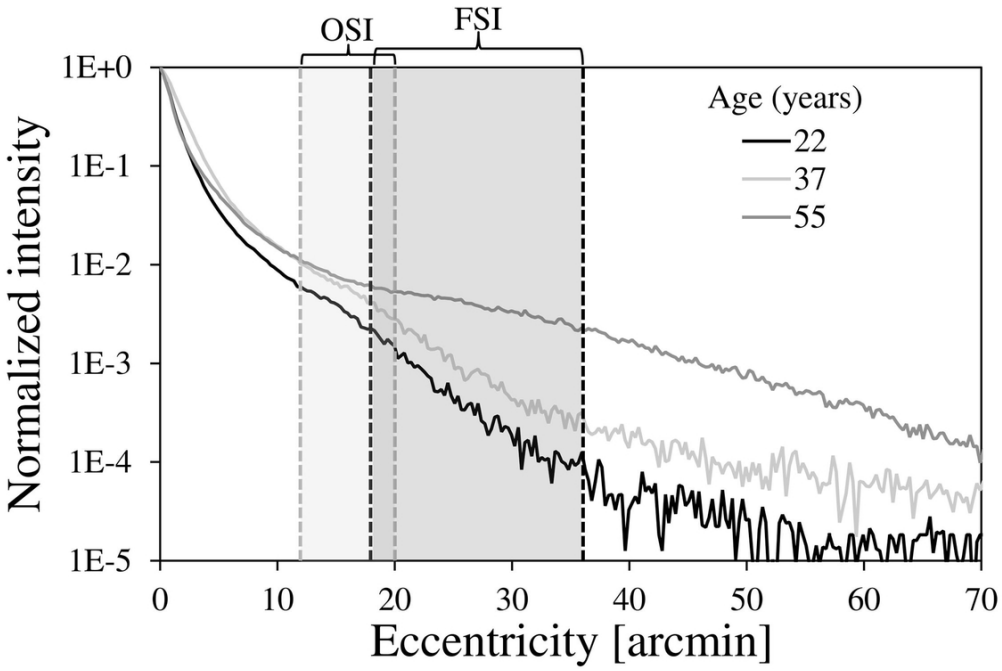

Figure 1. Normalized intensity in logarithm scale of the radial profiles of double-pass images for three subjects of 22 (black), 37 (light grey), and 55 (dark grey) years recorded with a commercial double-pass system. The region between grey dashed lines is used by the objective scatter index (OSI) and the region between black dashed lines is used by the frequency scatter index (FSI).

94x62mm (300 x 300 DPI)

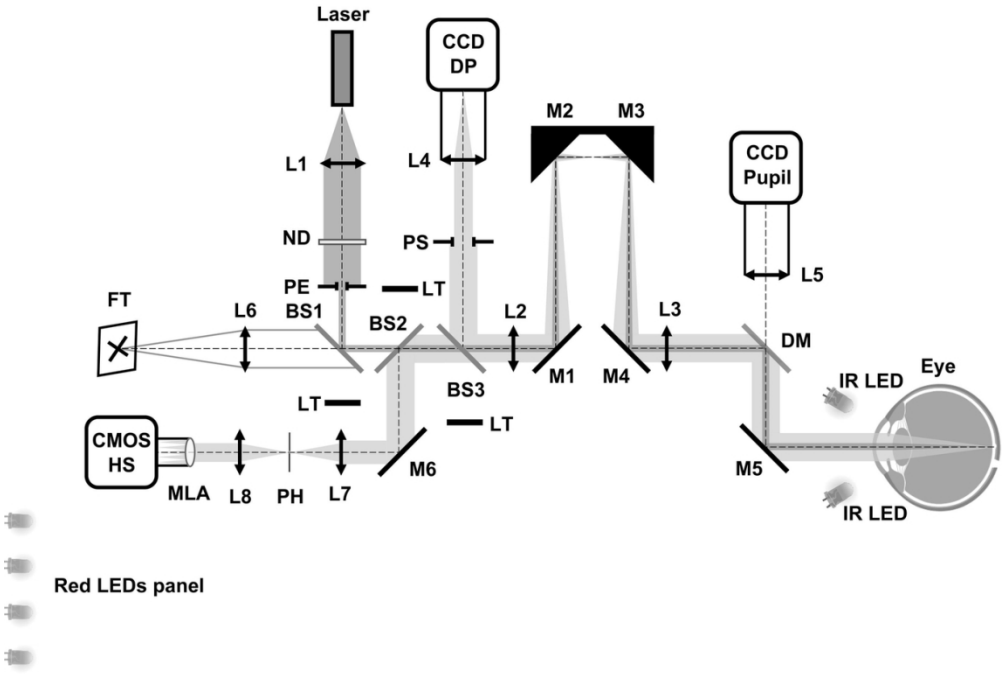

Figure 2. Layout of the double-pass setup to analyze the impact of aberrations. PE, entrance pupil; PS, exit pupil; BS, beam splitter; L, lens; M, mirror; Laser, laser diode; CCD, CCD camera; CMOS, CMOS camera; MLA, microlens array; DM, dichroic mirror; ND, neutral filter; FT, fixation test; PH, pinhole; LT, light trap; IR LED, Infrared light-emitting diode. In dark grey, the optical path of the first pass; in light grey, the optical path of the second pass.

117x80mm (300 x 300 DPI)

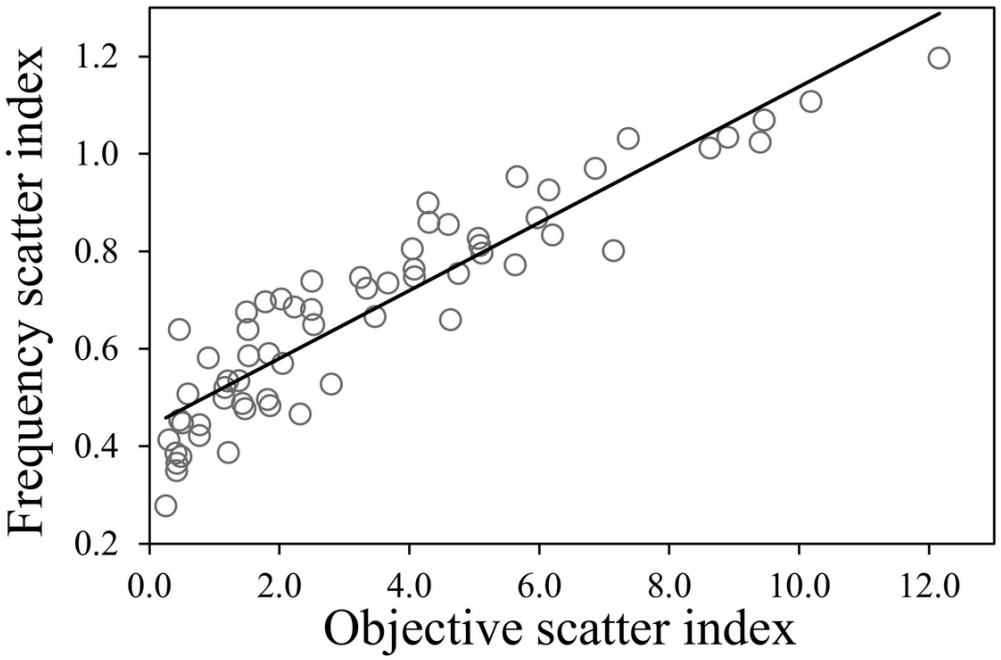

Figure 3. Dispersion diagram for the frequency scatter index versus the objective scatter index. Data correspond to subjects with diagnosed nuclear cataracts and subjects of the control group. The straight line was fitted through least squares (R^2=0.85).

94x61mm (300 x 300 DPI)

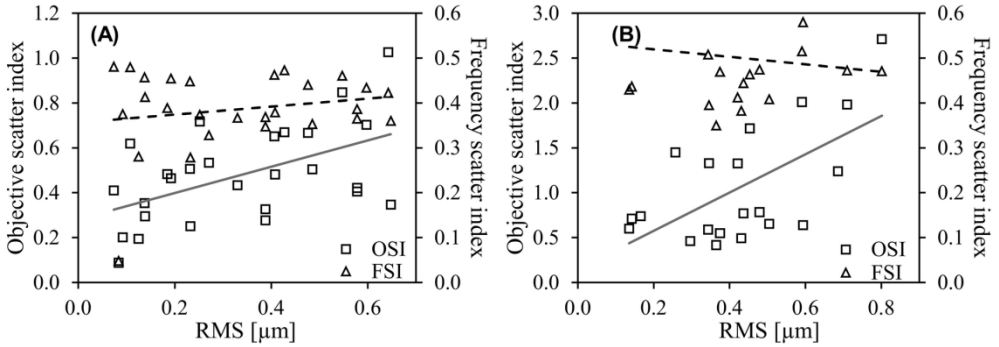

Figure 4. Objective scatter index (OSI) and frequency scatter index (FSI) as a function of the RMS of the wavefront when the pupil size increases (A) and when the eccentricity increases (B). Squares correspond to OSI and triangles to FSI. The straight line is a fit through least squares.

169x60mm (300 x 300 DPI)

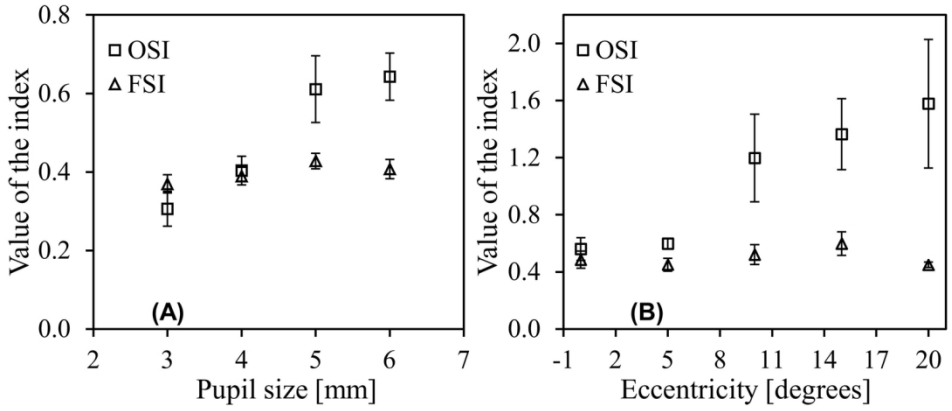

Figure 5. Mean value of the objective scatter index (OSI, squares) and frequency scatter index (FSI, triangles) for each pupil size (A) and eccentricity (B) evaluated in normal subjects. Error bars correspond to standard error.

149x61mm (300 x 300 DPI)